# Strained Si NMOSFETs for High Performance CMOS Technology

K. Rim, S. Koester, M. Hargrove\*, J. Chu, P. M. Mooney, J. Ott, T. Kanarsky\*, P. Ronsheim\*, M. Ieong\*, A. Grill, H.-S. P. Wong

IBM T. J. Watson Research Center, Yorktown Heights, NY; \*IBM Microelectronics Division, Hopewell Junction, NY phone: 914-945-2946 e-mail: rim@us.ibm.com

#### Abstract

Performance enhancements in strained Si NMOSFETs were demonstrated at  $L_{eff}$  <70 nm. A 70% increase in electron mobility was observed at vertical fields as high as 1.5 MV/cm for the first time, suggesting a new mobility enhancement mechanism in addition to reduced phonon scattering. Current drive increase by  $\geq$ 35% was observed at  $L_{eff}$  <70 nm. These results indicate that strain can be used to improve CMOS device performance at sub-100 nm technology nodes.

### Introduction

Due to the lattice mismatch, a pseudomorphic layer of Si on relaxed SiGe is under biaxial tensile strain, (Fig. 1) which modifies the band structure and enhances carrier transport [1]. In an electron inversion layer, the subband splitting is larger in strained Si because of the strain-induced band splitting in addition to that provided by quantum confinement (Fig. 2). The ground level splitting  $(E_0(\Delta_4) - E_0(\Delta_2))$  in a MOS inversion layer at 1 MV/cm transverse field is ~120 and ~250 meV for unstrained and strained Si, respectively. The increase in energy splitting reduces intervalley scattering and enhances NMOSFET mobility, as demonstrated at low (<0.6 MV/cm) [2, 3] and higher (~1 MV/cm) vertical fields [4]. The scaled device  $g_m$  is also improved due to the reduced density of states and enhanced non-equilibrium transport [5].

In this work, we fabricated strained Si NMOSFETs with sub-70 nm  $L_{eff}$ . These devices exhibited enhanced mobility at vertical fields as high as ~1.5 MV/cm and increased current drive, indicating promise for the 70 nm technology node.

#### **Device Fabrication**

Strained Si and relaxed SiGe layers were grown epitaxially by UHVCVD. The Ge content was graded in steps to form a fully relaxed SiGe buffer layer before a thin (~20nm) strained Si channel layer was grown. XRD analysis was used to quantify the Ge content (15, 20%) and strain relaxation in the SiGe layer. (Fig. 3 shows an example with 13% Ge content.) The strain state of the Si channel layer was confirmed by Raman spectroscopy. Fig. 4 shows a Raman spectrum of a strained Si layer on Si<sub>0.8</sub>Ge<sub>0.2</sub>, as grown and after 5 min. RTA at 1000°C. The strained Si peak position did not move after RTA, showing compatibility with the critical thermal cycles in a typical CMOS processes.

A standard CMOS process with STI isolation was used to fabricate the devices. Strained Si (SS) and unstrained Si control wafers were processed simultaneously using the same process condition. Fig. 5 shows the XTEM of a fabricated SS NMOSFET with  $L_{poly} = 110$  nm. A 2.2 nm gate oxide grown on strained Si had a uniform thickness and a smooth interface. Identical  $T_{ox}$  in the SS and control devices was confirmed by  $T_{inv}$  measurements, and resulted in comparable gate leakage characteristics. (Fig. 7.) Arsenic and phosphorus diffusion is enhanced in SiGe while boron diffusion is suppressed. This resulted in a larger gate overlap capacitance (Fig. 6) and a smaller  $L_{vol}$  for a given  $L_{pol}$ , in the SS devices.

## **Electrical Characterization**

The effective mobility  $\mu_{eff}$  is plotted as a function of vertical effective field  $E_{eff}$  in Fig. 8. Split C-V measurements were used to determine the inversion carrier concentration for the  $\mu_{\it eff}$  and  $E_{\it eff}$  calculations. The  $E_{\it eff}$  range is slightly higher for the SS devices due to suppressed boron diffusion in SiGe leading to higher channel doping. The  $\mu_{\text{eff}}$  of the SS device is well above the universal  $\mu_{eff}$ , and at least 70% higher than that of the control even at  $E_{eff} > 1 \text{ MV/cm}$ . In a technology employing  $T_{inv} \sim 1.5$  nm and  $V_{DD} \sim 1$  V, the maximum  $E_{eff}$  is not expected to exceed 1.5 MV/cm. The strain-induced  $\mu_{eff}$ enhancement in Fig. 8 persists for  $E_{eff}$  of up to and possibly beyond 1.5 MV/cm, demonstrating its relevance in the sub-70 nm technology nodes. The  $\mu_{eff}$  enhancement at such high  $E_{eff}$  cannot be explained by the improvement of phononlimited mobility  $\mu_{ph}$  [6] alone, and indicates that tensile strain may also improve the so-called surface roughness scatteringlimited mobility  $\mu_{SR}$  in NMOSFETs.

Figs. 9 and 10 compare SS and control devices with  $L_{eff} = 67 \text{ nm}$  as determined by a capacitance measurement technique. (A SS device with  $L_{poly} = 110$  nm was compared to a control device with  $L_{poly} = 80$  nm to account for the difference in gate overlap and match  $L_{eff}$ .) Narrow devices (W=0.28 µm) were compared to minimize the impact of selfheating [2, 4]. Excellent turn-off characteristics are observed with comparable subthreshold slopes (82 and 85 mV/dec) and DIBL (70 and 80 mV). The  $V_T$  of the SS device is lower (~200 mV) in part due to the smaller bandgap and lower conduction band in strained Si. No attempt was made to adjust or match the  $V_T$  of the SS and control devices. The smaller bandgap in SiGe and a finite density of epi dislocations lead to larger junction leakage in the SS devices, but not large enough to affect  $I_{off}$  for a typical choice of  $V_T$ . Fig. 10 shows the output current of the same devices shown in Fig. 9. For a gate over-drive  $V_{GT} = 0.8 \text{ V}$ , the current drive of the SS device is ~35% higher. At a lower  $V_{GT}$ , the enhancement is as large as 50%. The smaller output conductance in the SS device indicates a residual heating effect. When self-heating is completely suppressed, the current drive increase may be even larger.

 $G_{m,sat}$  vs. DIBL characteristics in Fig. 11 show that the performance enhancement in the SS devices persists for the devices with DIBL >80 mV and  $L_{eff}$  < 67 nm. The shortest  $L_{eff}$  plotted in Fig. 11 is 45 nm. These results indicate that the strained Si MOSFET is a promising device structure for high performance deep sub-100 nm CMOS technology.

## References

- [1] M. Fischetti and S. Laux, J. of Appl. Phys, 80, p. 2234, 1996.
- [2] J. Welser, et al., IEDM Tech. Dig., p. 947, 1994.
- [3] T. Mizuno, et al., Symp. on VLSI Tech., p. 210, 2000.
- [4] K. Rim, et al., IEDM Tech. Dig., p. 707, 1998.
- [5] K. Rim, et al., IEEE Trans. Elec. Dev., 47, p. 1406, 2000.
- [6] S. Takagi, et al., J. of Appl Phys., 80, p. 1567, 1996.

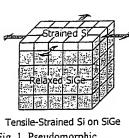


Fig. 1. Pseudomorphic, strained Si on relaxed SiGe.

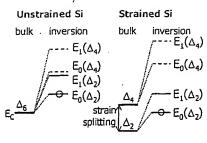
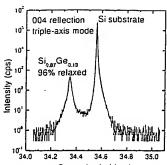


Fig. 2. Splitting of 6-fold degenerate Δ-valleys of conduction band in unstrained and tensile-strained Si inversion layer.



Bragg Angle (deg.)
Fig. 3. Triple-axis XRD data of a
typical strained Si/SiGe wafer.

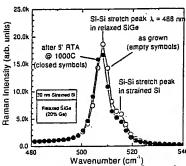


Fig. 4. Raman spectrum before and after RTA at 1000°C. No strain relaxation is observed.

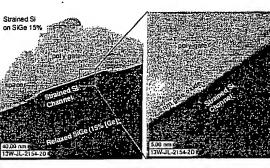


Fig. 5. XTEM of a completed strained-Si NMOSFET. Device region is free of dislocations. Good gate oxide quality with smooth interface is observed.

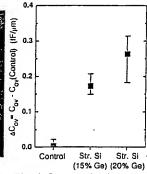


Fig. 6. Gate overlap is larger in SS devices due to enhanced As and P diffusion.

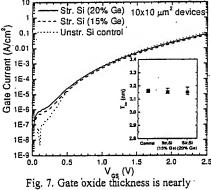


Fig. 7. Gate oxide thickness is nearly identical to control, resulting in comparable gate leakage.

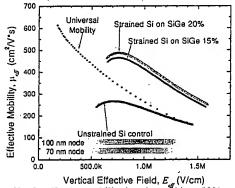


Fig. 8. Effective mobility is enhanced by >70% over the control and universal mobility even at a very high vertical field of >1.0 MV/cm.

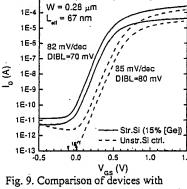
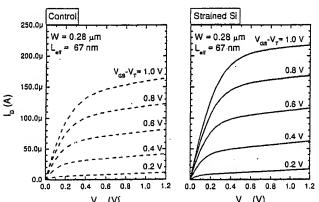


Fig. 9. Comparison of devices with  $L_{eff} = 67$  nm. Sub-threshold slopes and DIBL are comparable for SS and control.



 $V_{os}$  (V)  $V_{os}$  (V) Fig. 10. Output characteristics at equivalent gate over-drive for the devices shown in Fig. 9. Current drive enhancement is observed despite evidence of self-heating in the SS device.

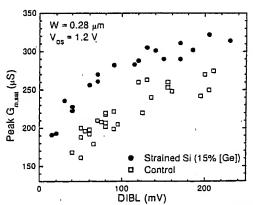


Fig. 11.  $G_m$  vs. DIBL indicates enhanced performance of strained Si devices across a range of channel lengths.